Performance evaluation of micromachined mirror arrays for adaptive optics

T. Weyrauch[a,b], M. A. Vorontsov[a], T. G. Bifano[c], A. Tuantranont[d], V. M. Bright[d], J. Karpinsky[e], J. Hammer[e]

[a)]U.S. Army Research Laboratory, Information Science and Technology Directorate, Adelphi, MD 20783
[b)]New Mexico State University, Klipsch School of Electrical & Computer Engineering, Las Cruces, NM 88003
[c)]Boston University, Manufacturing Engineering Department, Brookline, MA 02446
[d)]University of Colorado, Dep. of. Mechanical Engineering, Boulder, CO 80309
[e)]MEMS Optical, LLC, Huntsville, AL 35806

ABSTRACT

The performance of different MEMS mirrors from Boston University, MEMS Optical LLC, University of Colorado and OKO Technologies was studied in respect to an application in a model-free adaptive optics system. The frequency response characteristic was determined in a simple laser beam focusing set-up. Closed-loop adaptation experiments were performed using a VLSI controller system implementing a stochastic parallel gradient descent optimization algorithm. The system behavior using different MEMS mirror types, esp. adaptation speed, was compared.

Keywords: MEMS deformable mirrors, adaptive optics, stochastic parallel gradient descent

1. INTRODUCTION

Currently deformable mirrors based on micro-electromechanical systems (MEMS) technology attract much attention. They are supposed to replace conventional deformable mirrors esp. in adaptive optics systems with the advantage of higher resolution, lower power consumption and much less costs due to the use of well developed fabrication processes. Another advantage expected from this technology approach is an increase of mechanical bandwidth and thus higher operation frequencies. Several quite different approaches to realize MEMS deformable mirrors are known, but a comparison of their performance in a conventional adaptive optics system (based on wavefront measurements by a Shack-Hartmann sensor) is difficult, if not impossible, because each deformable mirror requires its own fine-tuned control system. This is different with an adaptive optics system using a model-free optimization strategy: A single, scalar beam quality metric, whose gradient is estimated after application of perturbation signals to the control channels, is optimized using an iterative gradient descent algorithm without any knowledge of the influence functions of the mirror actuators on the metric. With such an approach different MEMS mirrors may be compared in virtually the same system set-up. A certain disadvantage of model-free optimization is, however, the requirement of a higher number of iteration steps until wavefront distortions are corrected. Hence, the maximal achievable iteration rate of a system and therefore the dynamics of the MEMS mirrors is of special interest, esp. because sufficient fast controllers are available: Implementing a stochastic parallel gradient descent algorithm, a fast VLSI system (referred to as AdOpt controller) was developed recently by Johns Hopkins University and ARL[1]. It is scaleable to a large number of control channels due to its parallel system architecture and offers iteration rates up to the order of 10^5 s^{-1}. We used the AdOpt controller in a simple adaptive laser beam focusing set-up to study different MEMS mirrors in a closed loop system.

High-Resolution Wavefront Control: Methods, Devices, and Applications II, John D. Gonglewski, Mikhail A. Vorontsov, Mark T. Gruneisen, Editors, Proceedings of SPIE Vol. 4124 (2000) © 2000 SPIE. · 0277-786X/00/$15.00

2. MEMS MIRRORS UNDER INVESTIGATION

An overview of the working principles of the MEMS mirrors investigated in this study is presented in Fig. 1, where schematic cross-sections of the mirror elements are depicted. A more detailed description follows below.

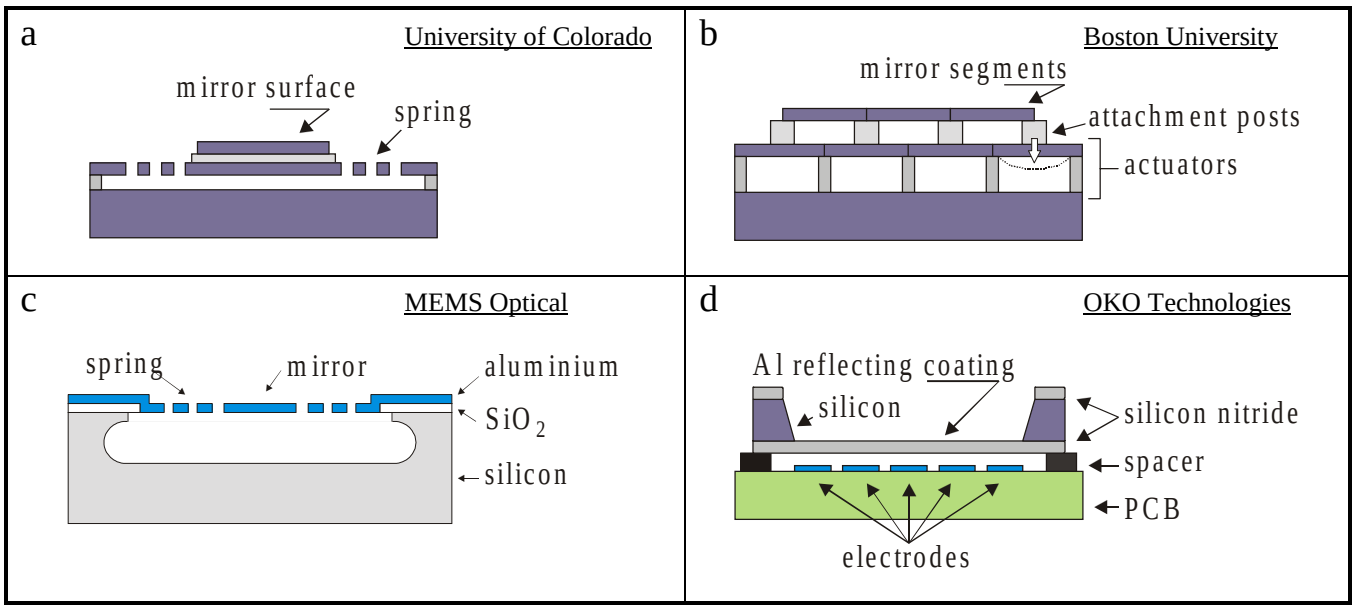

Figure 1. *Schematic of the working principle of the MEMS mirrors used for this study.*

University of Colorado (CU): The MEMS mirror from the University of Colorado (Boulder) was fabricated using the commercially available multi-user MEMS process (MUMPs) from MCNC[2]. It is a three layer surface-micromachining polycrystalline silicon (polysilicon) process. The mechanical structure is built from the two upper polysilicon layers: The 12 µm wide and 155 µm long flexures are etched from the center layer. Gold is deposited onto the top layer to from the 74 µm diameter mirrors. The mirror elements form a 12×12 array on a 250 µm grid with 128 active elements (2×2 elements in each corner are inactive). The deflection of the mirror elements is approximately dependent on the square of the applied voltage. Maximum deflection (at the threshold of the snap-through effect) is almost 1.4 µm. A major advantage of this MEMS deformable mirror is the low operation voltage. The snap-through effect occurs at 11.4 V. In order to have a reasonable fill factor, the mirror array was supplied with an lenslet array attached to the mirror chip[3]. Each circular microlens with a diameter of 250 µm is characterized by a hemispherical refractive index distribution; the focal length is 0.56 mm. A major drawback of such rectangular arrays of circular lenslets with a diameter equal to the mirror element distance is an inherent limitation of the fill factor. Additionally it is a very difficult task to provide good optical properties of the lenslet with a rather short focal length over its full aperture. In Fig. 2 an image of the (lenslet) surface of the CU mirror is shown. It demonstrates the small fill factor as the reflected light consists of distinct spots even not covering the full lenslet aperture. As a consequence of this behavior we observed strong diffraction into higher orders.

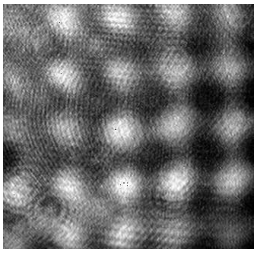

Figure 2. *Image of the lenslet array surface of the CU mirror*

Boston University (BU): MEMS deformable mirrors of Boston University were also fabricated at MCNC, but using besides the MUMPs also a custom-defined fabrication process to overcome some problems and restrictions, esp. to achieve a higher deflection and to avoid etching holes in the mirror surface. Despite some similarity in fabrication process, the basic concept of the Boston University MEMS mirrors is different from the UC design: The mirror surface is build from the 2 µm top polysilicon layer with a very high fill factor. The mirror membrane is supported by an underlying array of actuators via small 3 µm long attachment posts. Each actuators consists of a segment of the 2 µm thick center polysilicon layer anchored to a substrate along two opposite edges. The concept allows for both continuous membrane and segmented mirrors. Attaching the

supporting posts to the centers of the membrane segments gives piston type motion; if the corner of 4 adjacent segments are attached to one post one receives a hybrid type with piston and tip-tilt motion. The actuator design requires comparable high voltage in the range from 0 V to 200-300 V. Amplifier boards (26 channels each) matching the requirements of electrostatic driven devices were also designed by Boston University. Although several different mirror types were supplied by Boston University, in this study only a 4×4 segment (5×5 actuator) hybrid tip-tilt mirror was investigated.

MEMS Optical (MO): The deformable mirrors from MEMS Optical, Inc. are designed for low voltage operation. They have piston type motion and require a lenslet array to achieve a considerable fill factor. In contrast to the mirrors from University of Colorado the structure forming the springs and the mirror surface structure is built from an aluminum metal layer (1 μm thick). The gap below the metal layer (etched into silicon) is approximately 20 μm and allows for rather high deflections of up to 3 μm. We investigated two different types of mirrors (cf. Fig. 3): The first (MO1) has zig-zag shaped (or U shaped) springs and a mirror surface in form of a 160 μm wide octagon. It works with voltages in the range 0-15 V. Unfortunately, after installation of this mirror several elements were found to be broken (the damage was observable as rather large tilt of the mirror surface), which restricted the adaptation experiments and liability of their results. A second mirror (MO2) has spiral spring design and a smaller mirror surface. It requires higher voltages of about 30 V. Both mirrors have 6×6 elements with 500 μm center-to-center distance. They were used with the same diffractive lenslet array (back focal length 5.95 mm, designed for a wavelength of 633 nm but used with 690 nm), which was not attached to the mirrors but mounted on a 6-axis stage in front of the mirrors on variable holders for alignment. Each diffractive microlens has a square aperture, which allows for almost 100 % fill factor. The relative large surface of an individual mirror element (160 μm diameter) of the mirror with the zig-zag springs (MO1) made positioning of the lenslet array comparable easy but was much more difficult in case of the spiral spring mirror (MO2) because of the small effective mirror area. Due to the design of the mirrors there is a negligible correlation between the phase shift from neighbor mirror elements. This is demonstrated by the interferogram as well as the focal plane image shown in Fig. 4a,b, which are measured without application of voltage to the MO2 mirror elements. In closed loop experiments (cf. Fig. 7 and description below) the mirror elements were aligned and the interferogram showed a regular structure (Fig. 4c). Also a regular diffraction pattern in the focal plane appeared. However diffraction into higher orders was comparable low, the central spot in Fig. 4d is highly saturated in order to have visible higher diffraction orders.

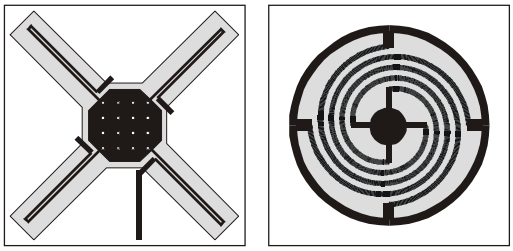

Figure 3. *Zig-zag shaped (MO1) and spiral (MO2) shaped spring design of MEMS Optical mirrors (left and right, respectively). Grey shade represents the outline of the etching holes.*

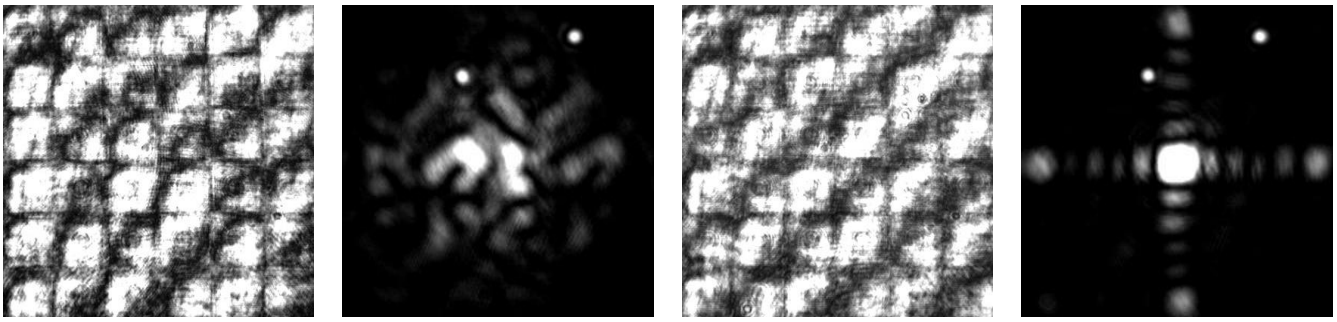

a **b** **c** **d**

Figure 4. *Interference pattern and focal plane images of the MO2 mirror with lenslet array without voltages applied to the actuators (a, b, respectively) and after optimization in a closed loop system (c, d, respectively).*

OKO: The micromachined deformable mirror from OKO Technologies has a continuous membrane from silicon nitride covered with an aluminium metal layer and suspended on the edges of a window etched into silicon. The electrode structure (37 hexagonal ordered electrodes with a center-to-center distance of 1.75 mm) is formed by a patterned metal layer on a PCB. The actuators require high voltage (≈ 200 V); maximal deflection at the center of the mirror is 9 μm. A major disadvantage of this mirror concept is, that application of a voltage to a single actuator influences the whole membrane. Thus, due to the

strong coupling between the actuators and the nonlinear response control of the mirror surface is in general a multidimensional nonlinear problem. However, this difficulty doesn't appear in case of model-free optimization.

Table 1. *Overview of some basic properties of the MEMS mirrors under investigation*

Mirror	Type of motion	Actuator distance	No of actuators	Mirror size	Actuator voltage
MEMS Optical 1 (zig-zag springs)	Piston w/lenslet	0.5 mm (rectangular)	36	3×3 mm^2	0 - 15 V
MEMS Optical 2 (spiral springs)	Piston w/lenslet	0.5 mm (rectangular)	36	3×3 mm^2	0 - 30 V
University of Colorado	Piston w/lenslet	0.25 mm (rectangular)	128 (36 used)	3×3 mm^2	0 - 11 V
Boston University	Segmented tip-tilt-piston	0.25 mm (rectangular)	25	1×1 mm^2	0 - 300 V (0 - 10 V)*
OKO	Continuos membrane	1.75 mm (hexagonal)	37	$\varnothing$ = 15 mm	0 - 210 V (0 - 4.5 V)*

(* Amplifier input)

3. FREQUENCY RESPONSE CHARACTERISTIC OF THE MEMS MIRRORS

For measurement of the dynamic properties of the MEMS mirrors a laser beam reflected from the mirror was focused onto a pinhole (cf. Fig. 5). The laser power emergent from the pinhole was measured with a photosensor (photomultiplier and amplifier module) and corresponds to the system performance metric J of an adaptive focusing system. A part of the mirror actuators was connected to a function generator, applying a sinusoidal voltage $\Delta U(\nu)$ and a d.c offset voltage U_0. The other mirror actuators were held at ground level. If the amplitude $\Delta U(\nu)$ is sufficiently small and the offset adjusted properly the sinusoidal deformation of the mirror surface induces also a variation $\Delta J(\nu)$ of the metric at the same frequency. Its amplitude in dependence on the frequency ν characterizes the response of the mirror. Results of measurements are presented in Fig. 6.

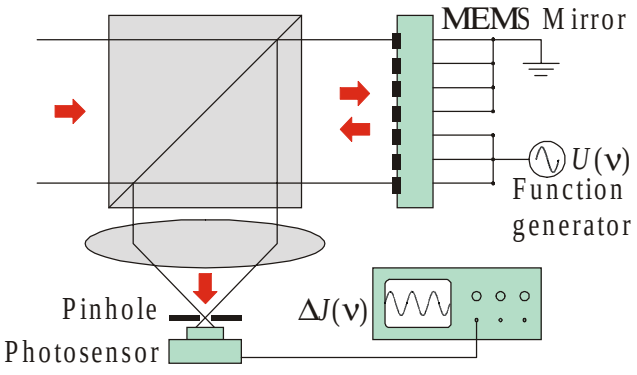

Figure 5. *Set-up for measurement of dynamic properties of MEMS mirrors*

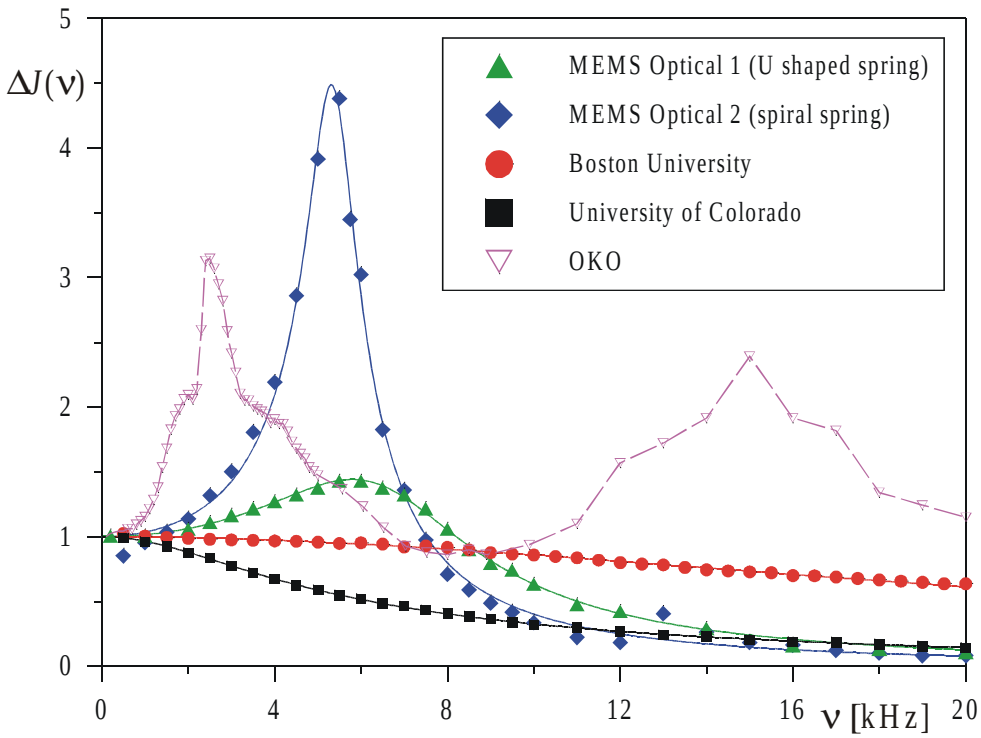

Figure 6. *Metric oscillation amplitude $\Delta J(\nu)$ for different MEMS mirrors. Straight lines are according equation 4 with parameters ΔJ_0, ν_0 and s obtained from least-square fits. Both, measured and fitted data are normalized by the respective parameter ΔJ_0 (see discussion below).*

In order to discuss the results we may describe the behavior of the mirror elements in a simple mechanical model as a damped oscillator

$$\frac{d^2x}{dt^2} + s\frac{dx}{dt} + \omega_0^2 x = \frac{F(t)}{m} \quad , \tag{1}$$

where x is the deflection, s is the damping constant, $\omega_0 = \sqrt{k/m}$ is the resonance frequency of the non-damped mechanical equivalent system with the spring constant k and the mass m. $F(t)$ is a time dependent external force. For electrostatic actuators we can with quite good approximation consider quadratic dependence of this force on the applied voltage, i. e. $F(t) = aU^2(t)$. Thus for a d.c. offset voltage U_0 and a sinusoidal time dependent component $\Delta U \exp(i2\pi\nu t)$ with small amplitude we have

$$F(t) = a\left[U_0 + \Delta U \exp(i2\pi\nu t)\right]^2 = a\left[U_0^2 + 2U_0\ \Delta U \exp(i2\pi\nu t) + \Delta U^2 \exp(i4\pi\nu t)\right] \tag{2}$$

One may neglect the terms quadratic in U_0, which gives a constant offset, and ΔU, which gives a very weak oscillation at the double frequency 2ν, and consider only the term with the excitation frequency ν. With a linear relationship between deflection x and metric oscillation ΔJ (provided by an appropriate choice of U_0) one receives

$$\frac{d^2J}{dt^2} + s\frac{dJ}{dt} + \omega_0^2 J = b\,\Delta U \exp(i2\pi\nu t) \quad , \tag{3}$$

i. e. again the well-known differential equation for a damped oscillator with the steady-state solution for the driven oscillation amplitude

$$\Delta J(\nu) = \frac{\Delta J_0}{\sqrt{\left(1-\nu^2/\nu_0^2\right)^2 + \left(s\nu/\nu_0^2\right)^2}} \tag{4}$$

Fitting this equation to each set of measured data one receives the parameters ν_0 and *s*, which characterize the response characteristics in frames of the model. The resulting fitting parameters are presented in Table 2; the straight lines in Fig. 6 are calculated according to Equation 4 with the corresponding parameters. The measured data of the OKO mirror didn't allow to use this simple model, because several close resonance peaks were found. Resonance frequency and damping constant of the lowest frequency resonance were estimated from position and height of the corresponding peak. Multiple resonances were observed because the measurements don't represent the properties of a single actuator but of the whole membrane, able to oscillate in different modes. The mirrors of MEMS Optical show also distinct resonance maximums. The mirror with the spiral springs (MO2) has a slightly lower resonance frequency ν_0 = 5.4 kHz than the MO1 mirror with the zig-zag design (6.8 kHz) and is much less damped. The curve $\Delta J(\nu)$ of the mirror from the University of Colorado decreases monotonically and shows no resonance maximum, corresponding to a damping constant s/ν_0 = 3.0 above the critical value 2. The best frequency range is offered by the BU mirror. However, in the frequency range above 20 kHz the limited frequency range of the sensor module influenced strongly the result. Thus the fitting parameters probably represent rather the behavior of the amplifier within the sensor module than the mirror properties. However, the mirrors are at least as fast as the measurements imply.

Table 2. *Fitting parameters for the frequency response curves*

Mirror	Resonance ν_0 / kHz	Damping s/ν_0
MEMS Optical 1 (zig-zag)	6.8	0.75
MEMS Optical 2 (spiral)	5.4	0.22
University of Colorado	9.8	3.0
Boston University	(28)*	(2.1)*
OKO	$2^{\#}$	$0.4^{\#}$

* Measurements limited by sensor module; # Resonance with lowest frequency (approximated data)

4. CLOSED LOOP PERFORMANCE

Model free optimization with stochastic parallel gradient descent algorithm

For investigation of the closed loop performance of the MEMS mirrors we used a simple laser beam focusing system and a model-free optimization strategy. Instead of measurement of the wave-front a single scalar metric *J* is used to describe the system performance. In our case it is chosen as the power emergent from a pinhole (50 µm diameter) placed in the focal plane of the focusing lens and represents the Strehl ratio (cf. Fig. 7a). Model-free optimization was performed using a stochastic parallel gradient descent algorithm. The peculiarity of this optimization strategy is, that a set of stochastic perturbation voltages $\delta\vec{u} = (\delta u_1, \ldots, \delta u_j, \ldots, \delta u_N)$ is applied simultaneously in parallel to the set of voltages $\vec{u} = (u_1, \ldots, u_j, \ldots, u_N)$, which controls the actuators of the MEMS mirror. The perturbation voltages δu_j have equal absolute values but random sign. After application of one set of perturbation voltages $\delta\vec{u}$ the corresponding perturbed metric value $J_+^{(n)}$ is measured. Then the sign of each perturbation voltage δu_j is changed and the perturbed metric $J_-^{(n)}$ is measured, i. e.

$$J_{\pm}^{(n)} = J(u_1^{(n)} \pm \delta u_1, \ldots, u_j^{(n)} \pm \delta u_j, \ldots, u_N^{(n)} \pm \delta u_N) \ . \tag{5}$$

After calculation of the metric perturbation as the difference of the two perturbed values

$$\delta J^{(n)} = J_+^{(n)} - J_-^{(n)} \tag{6}$$

it is used to update the control voltages according to the rule

$$u_j^{(n+1)} = u_j^{(n)} + \gamma \delta J^{(n)} \operatorname{sign}(\delta u_j) \ . \tag{7}$$

Here γ is a gain factor (to be chosen properly), which determines the size of the control voltage correction.

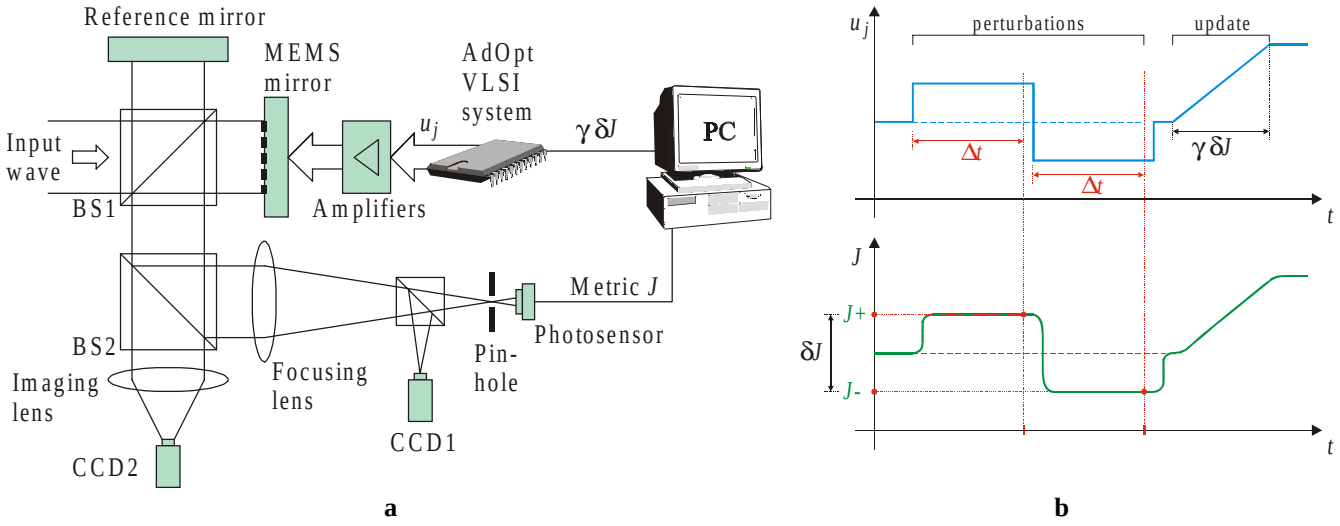

Figure 7. *a) Schematic of the adaptive laser beam focusing system. b) Schematic of the evaluation of a control voltage channel u_j and the metric J during one iteration cycle.*

Fig. 7b demonstrates the evaluation of the voltage of one control channel and the metric during one iteration cycle schematically. A major advantage of this algorithm is the possibility of its implementation in very large scale integrated (VLSI) circuits, which allows for very fast parallel control. The AdOpt VLSI controller chip, recently developed at Johns Hopkins University and ARL[1], provides simultaneously 19 control voltages u_j and allows for a scaleable system architecture. The chip implements the application and generation of pseudo-random perturbation voltages δu_j, as well as the control signal update. A PC with digital and analog I/O boards provides clocking signals, the measurements of the metric signal and controls some system parameters. It also delivers the sign of the metric change and an update pulse with a variable length proportional to $|\gamma\delta J^{(n)}|$ to the AdOpt chips, which calculate the full update term $\gamma\delta J^{(n)}\operatorname{sign}(\delta u_j)$ for each channel.

Comparison of the maximal achievable iteration rate

The closed loop performance of an adaptive laser beam focusing system comprising the MEMS mirrors and the AdOpt VLSI controller was evaluated by means of testing its ability to induce wave-front distortions and to correct them. Switching between metric maximization (correction of distortions) and minimization (self induction of distortions) is possible by changing the sign of the update gain coefficient γ.

As MEMS mirrors are expected to work at higher rates than conventional deformable mirrors, special attention was paid to the maximal achievable iteration rate. A comprehensive study of the system with the OKO mirror was already reported[4], a

system using the 5×5 actuator mirror from Boston University is discussed in more detail in this volume[5]. The iteration rate was controlled by variable delays Δt between the application of the perturbation voltage and the measurement of the corresponding perturbed metric value (cf. Fig. 7b). The OKO mirror worked until about 1500 s^{-1}. The Boston University mirror was used until 5900 s^{-1}. Latter rate was achieved with zero delays and was thus limited by the speed of the control computer and the I/O boards used in the experiments. A variation of the delays length Δt did not change the performance of the system with the BU mirror: The adaptation speed (in terms of maximal metric change per iteration step, i. e. $J'_{max} = (dJ/dn)_{max}$) did not depend on the delay Δt. Further experiments were performed using both mirrors from MEMS Optical. The maximal working iteration rate was about 4000 s^{-1} in both cases. The behavior changed significantly when the delays were chosen larger than required for the limit. A slower iteration rate could even lead to worse performance of the system. This behavior was more pronounced for the MO2 mirror, where delays up to several hundred μs influenced the behavior, whereas in case of the MO1 mirror delays larger than about 150 μs didn't change the system behavior.

For an interpretation of these observations one should consider the response of the mirror elements to a step-like voltage change as it is applied for the perturbation voltages. Since the step response is related to the frequency response (Fig. 6), in frames of the simple model of damped oscillators we can use the parameters ω_0 and s, obtained from fitting as described above, to calculate the step response function. We may distinguish two important cases: For overcritical damping ($s/\omega_0 > 2$), the response function is a sum of a constant C (the value for $t \to \infty$) and two exponential decay functions

$$x = A\exp(-t/\tau_1) + B\exp(-t/\tau_2) + C \text{, with } \tau_{1,2} = \left(\frac{s}{2} \pm \sqrt{\frac{s^2}{4} - \omega_0^2} \right)^{-1}, \tag{8}$$

where the larger time constant is at least $\tau > 2/s$. In case of undercritical damping the function is a damped oscillation with an oscillation frequency ω and an envelope exponential decay with a time constant τ, i. e.

$$x = \exp(-t/\tau)\left[A\cos\omega t + B\sin\omega t\right] + C \text{, with } \omega = \sqrt{\omega_0^2 - \frac{s^2}{4}}, \ \tau = 2/s. \tag{9}$$

Curves calculated for a step response from 0 to an equilibrium value x_{inf} using the fit parameters for different mirrors are presented in Fig. 8. The OKO mirror is not considered here, because its multi-frequency response of the membrane doesn't allow to use this simple approach. The comparable fast relaxation of the Boston University mirror allows to reach the equilibrium values for the perturbation voltages during a iteration cycle of about 170 μs (corresponding to the maximal iteration rate). The MEMS Optical mirror (MO2 - spiral springs) doesn't reach an equilibrium value within 250 μs, the cycle duration corresponding to the rate of 4000 s^{-1}. This induces errors in the gradient estimation because perturbed metric values can't be measured properly as well as a general "noisy" behavior. Thus one must expect a loss in performance, which was indeed found in our experiments: The maximal adaptation speed (metric change per iteration J'_{max}) was at least 5 times smaller than in case of the Boston University mirror. The MO1 mirror with zig-zag springs showed an intermediate behavior, but problems because of the several damaged elements do not allow for a direct comparison. The mirror from the University of Colorado has not yet been investigated in connection with the AdOpt VLSI controller and no data for maximal iteration rate are available. From the response curve in Fig. 6 we should expect to achieve a rate comparable to the MEMS Optical mirrors. The curves in Fig. 8 explain also another observation: The mirrors from MEMS Optical, especially the spiral spring mirror, needed significantly smaller perturbation voltages to achieve the same metric perturbation as in case of the BU mirror. This is related to the overshooting due to the oscillatory nature of the response. It should be noted, that metric oscillations were observable directly using an oscilloscope. However, the actual shape depends strongly on whether the system is at an maximum or in an intermediate state.

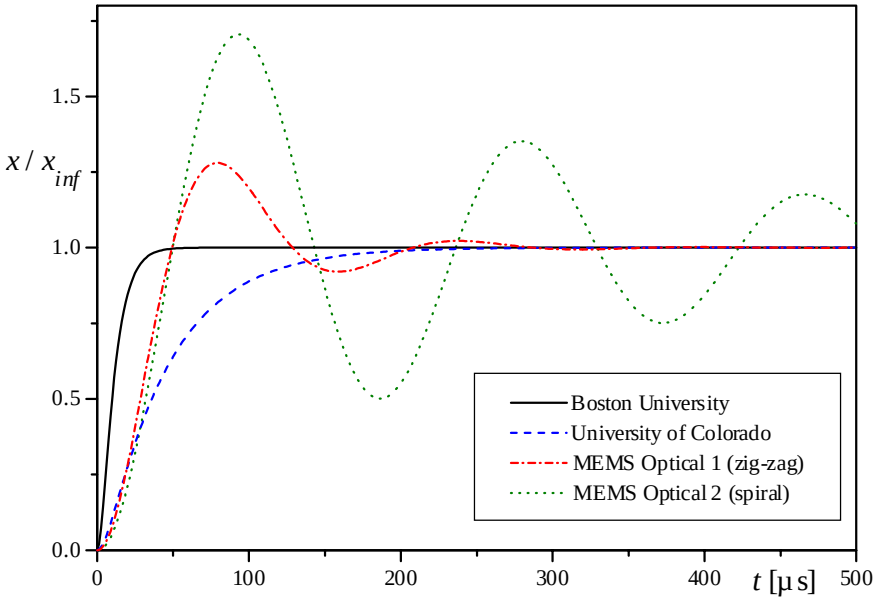

Figure 8. *Step response functions for the different mirrors calculated according to the parameters given in Table 2.*

Actuator sensitivity curves

In contrast to tip-tilt mirrors a phase shift corresponding to one wavelength λ doesn't change the system performance metric *J* in case of piston type movement. This can be seen from measurements of the metric *J* when varying the voltage of one single actuator. Fig. 9a shows such sensitivity curves for four selected actuators of the MO2 mirror (spiral springs). The maximums of a single curve have the same value (and are thus global), whereas in case of the tip-tilt mirror only one global maximum exists[5]. Thus, assuming an unlimited range of actuator stroke, the system should be able to find equivalent maximums independent from starting conditions. This may not apply in general for a limited range of mirror deflection, but we found system parameters, where indeed only one single (global) maximum exists. To demonstrate this we performed several minimization-maximization experiments and determined the distribution of metric values measured after maximization. One corresponding histogram is presented in Fig. 9b. It was evaluated from 1000 iteration steps and 200 trials; the metric values were measured in intervals of size 0.01.

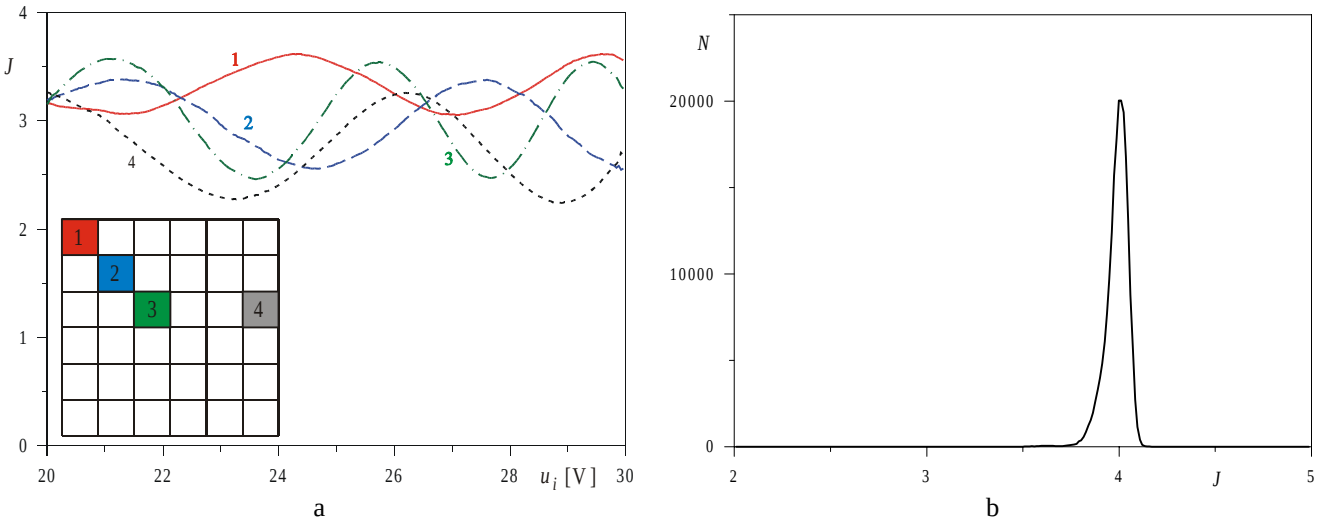

Figure 9. *a) Dependence of the metric J on the voltage of selected mirror elements of MEMS Optical MO2 mirror (the inset demonstrates the position of the elements within the mirror array. b) Histogram for metric values J measured after maximization*

5. ACKNOWLEDGMENT

This work was performed at ARL's Intelligent Optics Laboratory in Adelphi, MD, in frames of a cooperation project with the New Mexico State University with financial support by the Air Force Office of Scientific Research (contract number F49620-99-1-0342) The authors would like to thank Gary W. Carhart and Marc Cohen for their assistance in preparing the computer software and the AdOpt VLSI controller circuit used for the presented experiments.

6. REFERENCES

1. R. T. Edwards, M. Cohen, G. Cauwenberghs, M. A. Vorontsov, G. W. Carhart, "Analog VLSI Parallel Stochastic Optimization for Adaptive Optics", in *Learning on Silicon*, eds. G. Cauwenberghs, M. A. Bayoumi, (Kluwer Academic Publishers, Boston, Dordtrecht, London, 1999), Chapter 16, pp. 359-382.
2. D. A. Koester, R. Mahadevan, and K. W. Markus, "Multi-user MEMS process (MUMPs): Introduction and design rules. rev. 4", Technical Report MCNC MEMS Technical applications center. 3021 Cornwallis Road, Research Triangle Park, NC 27709 (1996).
3. A. Tuantranont, V. M. Bright, W. Zhang, and Y. C. Lee, "Flip Chip Integration of Lenslet Array on Segmented Deformable Micromirrors", in *Design, Test, and Microfabrication of MEMS and MOEMS*, Proc. SPIE **3680**, Eds. B. Courtois, S. B. Crary, W. Ehrfeld, H. Fujita, J.-M. Karam, K. W. Markus, pp. 668-678 (1999).
4. M. A. Vorontsov, G. W. Carhart, M. Cohen, and G. Cauwenberghs, "Adaptive optics based on analog parallel stochastic optimization: analysis and experimental demonstration", *J. Opt. Soc. Am. A.* (August 2000).
5. T. Weyrauch, M. A. Vorontsov, T. G. Bifano, and M. K. Giles, "Adaptive optics system with micromachined mirror array and stochastic gradient descent controller", *this volume*.